



## **Utilizing Computational Fluid Dynamics (CFD), Analyse the Heat Transfer and Fluid Flow in A Shell and Tube Heat Exchanger Using Molten Salt-Based Nanofluid.**

*Sushil Kumar Yadav<sup>1</sup>, Prof. Animesh Singhai<sup>2</sup>*

<sup>1</sup> Research Scholar, Trinity Institute of Technology and Research, RGPV Bhopal, MP, INDIA

<sup>2</sup> Professor, Trinity Institute of Technology and Research, RGPV Bhopal, MP, INDIA

### **ABSTRACT**

With the aid of ANSYS Fluent, thermal and flow behaviour of a molten salt-based nanofluid in turbulent sections of a shell and tube heat exchanger was numerically analysed. Water was used as the study's base fluid and nanoparticles with a diameter of twenty (20) nm were used. To investigate the impacts on heat transfer coefficient, pressure drop, and nanofluid thermal and hydrodynamic behaviour, the nanofluid was simulated at three distinct particle loadings (ranging from 0.1 to 1% vol) and under three sets of Reynolds numbers (between 15,000 and 70,000). Both the rate of heat transfer and pressure drop were found to be improved by raising the particle loading and Reynolds number.

In this analysis, a 3-dimensional numerical (3-D) simulation was used to examine the forced convection heat transfer of the molten salt nanofluid  $\text{KNO}_3\text{-Ca}(\text{NO}_3)_2 + \text{SiO}_2$  and  $\text{KNO}_3\text{-Ca}(\text{NO}_3)_2 + \text{TiO}_2$  in a circular tube. The heat transmission physiognomies of a  $\text{KNO}_3\text{-Ca}(\text{NO}_3)_2 + \text{SiO}_2$  and  $\text{KNO}_3\text{-Ca}(\text{NO}_3)_2 + \text{TiO}_2$  molten salt nanofluid in a circular tube were studied using the simulation tool ANSYS 19.2.

The main objectives of the present work are as follows to investigate the impacts on heat transfer coefficient, pressure drop, and nanofluid thermal and hydrodynamic behavior. Also examine the thermal properties of the molten salt nanofluid in a circular tube,  $\text{KNO}_3\text{-Ca}(\text{NO}_3)_2 + \text{SiO}_2$  and  $\text{KNO}_3\text{-Ca}(\text{NO}_3)_2 + \text{TiO}_2$  and Parameters like the Nusselt number and heat transfer coefficient are used to study the effect of  $\text{TiO}_2$  nanoparticles on the thermal properties of molten salt

**Keywords:** Molten salt nanofluid, nanoparticles, Heat transfer, CFD.

### **I. INTRODUCTION**

A heat exchanger is an apparatus that enables the energy transfer between one or more fluid streams where there is already a temperature differential. Depending on the kind of chemical process industry, heat exchangers are used to provide efficient and adequate heat transfer for cooling, heating, and material phasing shift (Devi & Nagamani, 2015). Chemical process industries include power generation, petrochemical, and heat recovery systems. Shell and tube heat exchangers are indirect contact devices that use conduction and convection to transfer heat as the fluids go through the bundles of shell and tubes individually (Othman, 2009). These heat exchangers are made with a variety of adaptable variants to produce the ideal heat load. In order to enhance the surface area for heat transfer, geometric characteristics (such as diameter, length, and number of tubes, etc.) can be changed, however fluid flow has a substantial impact on performance variables like the rate and efficiency of heat transfer (Jadhav & Koli, 2014).

Molten salts are the material often employed for phase transition for thermal energy storage. Molten salts solidify into a liquid at ambient temperature and atmospheric pressure by transmitting thermal energy to the storage environment. In the majority of molten salt energy storage devices, the molten salt is kept as a solvent during the energy storage process. Molten salts melt at a temperature of around 220°C and generally include 60% sodium nitrate and 40% potassium nitrate.

### **II. LITERATURE REVIEW**

Over the past two decades, research involving molten salts has become more and more popular as working fluids for high temperature processing applications and thermal-fluidics applications due to their stability at elevated temperatures, low vapour pressures, broad operating temperature ranges, minimal environmental footprint, ease of materials handling, low material costs, and safety. Molten salts are used as engineering fluids in a variety of applications, including energy storage, advanced nuclear reactors, chemical reprocessing, and solar power production.

**Patricia Anne D. Cruz, Ed-Jefferson E. Yamat et al. (2022)** Numerical analysis of the thermal and flow behavior of CuO-water nanofluid under turbulent regions in a shell and tube heat exchanger was conducted using ANSYS Fluent. Twenty-nine (29) nm diameter CuO nanoparticles, and water as base fluid were used in the study. The nanofluid was simulated at different particle loading (0.1 to 1% vol), and under three sets of Reynolds number

(ranging from 17,000 to 71,000), to study the effects on heat transfer coefficient, pressure drop, and nanofluid thermal and hydrodynamic behavior. Increasing the particle loading and Reynolds number was found to enhance both the heat transfer rate and pressure drop. A maximum of 48% enhancement in the heat transfer was observed at the highest particle loading, but with the consequence of doubled pressure drop. Performance indices greater than 1 were attained for particle loading below 0.25% vol, regardless of the Reynolds number. The conditions that produced the highest index were at the lowest particle loading and lowest Reynolds number.[1]

**Yang et al. (2010)** the improved heat transfer from the spiral tube used in a Concentrated Solar Power (CSP) plant consumer was studied instead of a smooth tube.  $\text{KNO}_3\text{-NaNO}_2\text{-NaNO}_3$  (Mass Salt Hitec 53:7:40) is the ternary nitrate eutectics which were the operating solvent. Also used in the research section were a heated 316L Stainless Steel spiral fan. The test results show that, relative to the heat transfer efficiency of a smooth tube, the amount of Reynolds ranges from 15 000 to 55 000 by up to 3 times in one spiral tube [2].

**C.Anbumeenakshi, M.R.Thansekhar et al. (2017)** This present experimental study investigates the combined effect of nanofluid and non-uniform heating on the cooling performance of a microchannel heat sink. The microchannel heat sink considered in this study has evenly spaced 30 rectangular channels with a hydraulic diameter of 0.727 mm. Three separate heaters of identical dimensions are used in the experimental study. Non-uniform heating condition is provided by switching on any two of the three heaters at a time.  $\text{Al}_2\text{O}_3$ /water nanofluid of volume concentration 0.1% and 0.25% and deionized water are used as working fluid. Results show that  $\text{Al}_2\text{O}_3$ /water nanofluid of 0.25% volume concentration exhibit lower maximum surface temperature and average surface temperature than with  $\text{Al}_2\text{O}_3$ /water nanofluid of 0.1% volume concentration and water in uniform and non-uniform heating condition.

**Chatcharin Sitprasert, Pramote Dechaumphai et al. (2008)** The interfacial layer of nanoparticles has been recently shown to have an effect on the thermal conductivity of nanofluids. There is, however, still no thermal conductivity model that includes the effects of temperature and nanoparticle size variations on the thickness and consequently on the thermal conductivity of the interfacial layer. In the present work, the stationary model developed by Leong et al. (J Nanopart Res 8:245–254, 2006) is initially modified to include the thermal dispersion effect due to the Brownian motion of nanoparticles. This model is called the ‘Leong et al.’s dynamic model’. However, the Leong et al.’s dynamic model over-predicts the thermal conductivity of nanofluids in the case of the flowing fluid. This suggests that the enhancement in the thermal conductivity of the flowing nanofluids due to the increase in temperature does not come from the thermal dispersion effect.

**Arun Kumar Tiwari, Pradyumna Ghosh et al. (2015)** heat exchange device using nanofluid needs to operate at best nanoparticle loading to get the maximum heat transfer performance. In this paper, an attempt has been made to optimize different nanofluid particle volume fractions based on a maximum heat transfer rate, convective heat transfer coefficient, overall heat transfer coefficient, effectiveness and performance index. The novelty of the present study is the optimization of particle volume fraction of various nanofluids based on experimentation in the commercial plate heat exchanger for wide range of nanoparticle volume fraction (0–3%). Effects of other operating conditions on the optimization have been discussed as well. Results show that for maximum enhancement of heat transfer characteristics, different nanofluids work at different optimum volume concentrations. For  $\text{CeO}_2$ /water,  $\text{Al}_2\text{O}_3$ /water,  $\text{TiO}_2$ /water and  $\text{SiO}_2$ /water nanofluids, the optimum volume concentrations are 0.75%, 1%, 0.75% and 1.25%, respectively, at the flow rate of 3 lpm. The corresponding maximum heat transfer enhancements are about 35.9%, 26.3%, 24.1%, and 13.9%, respectively.

### III. GEOMETRY SETUP AND MODELLING

The geometry of the shell and tube heat exchanger (STHE) was based on the experimentally validated work of Patricia Anne D. Cruz et al. (2022), which was created in compliance with the standards of the Tubular Exchanger Manufacturers Association (TEMA).

where water is circulated in the shell and a molten salt nanofluid flows down the tube. In this experimental technique, the heat is transmitted from the base fluid (water) to the molten salt nanofluid heat exchanger.

**Table 1. STHE geometry design of casing heat exchanger**

Heat Exchanger length	600mm
Outer diameter (Tube)	20 mm
Outer diameter (Shell)	90 mm
No. of tubes	7
Number of baffles	6
Central Baffle spacing	86 mm
Tube bundle geometry	Triangular
Pitch 30 mm	30mm
Baffle inclination angle	0°
Nozzle Diameter	36mm

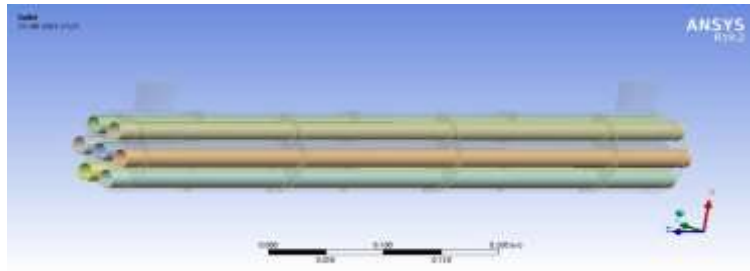


Figure 1. Computational model of heat exchanger.

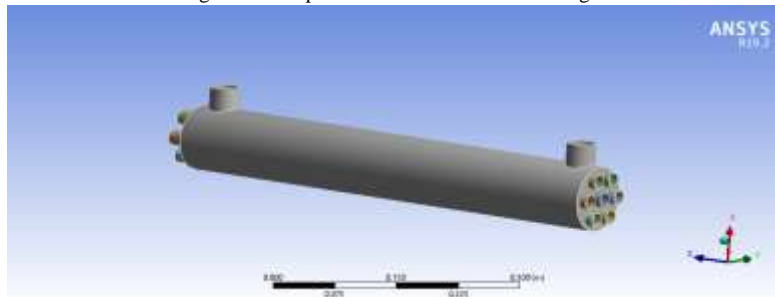


Figure 2. Isometric view of heat exchanger modal

In the pre-processor stage of ANSYS FLUENT R 19.2, a three-dimensional discretized model was created. The programmed ANSYS creates a coarse mesh, despite the fact that the grid types and simulation results are connected. The structure as a whole must be discrete in the final volume. Unit-size mixed cells (ICEM Tetrahedral cells) with triangular frontier faces make up the mesh. A mesh metric and a medium fluid curvature are employed in this investigation.

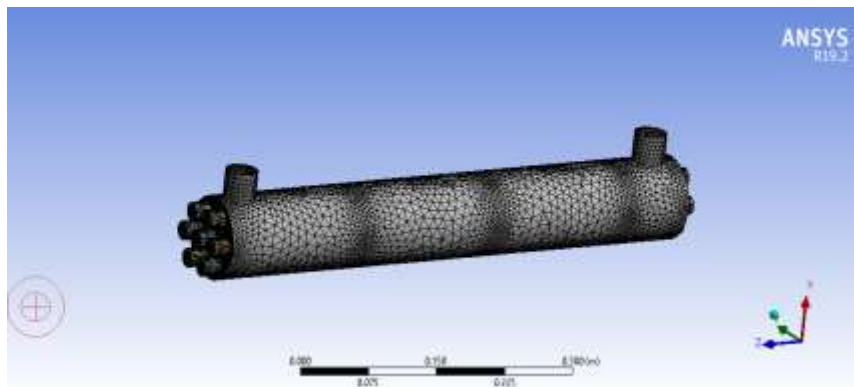


Figure 3. Meshing of heat exchanger.

Table 2. Meshing detail of model

S. No.	Parameters	
1	Curvature	On
2	Smooth	Medium
3	Number of nodes	293975
4	Number of elements	668861
5	Mesh metric	None
6	Meshing type	Tetrahedral

The Fluent 19.1 was used to calculate computationally. In research, the approach used to differentiate the governing equations was a finite element. A standard k-epsilon equation was used with flow and energy equations to solve turbulence. Which implies the following hypotheses:

- 1) There is negligence of thermal radiation and normal convection;
- 2) The average of fluid and solid properties is calculated
- 3) Flow is incompressible;
- 4) Heat transfer steady state;
- 5) Transitional fluid flow and turbulent regimes, and

- 6) The fluid is distributed uniformly between the channels and the inlet channels have a uniform velocity profile.

The numerical simulation was with a 3-Dimensional steady state turbulent flow system. In order to solve the problem, governing equations for the flow and conjugate transfer of heat were customized according to the conditions of the simulation setup.

**Table 3. Thermodynamic Properties of TiO<sub>2</sub> nanoparticles with 1 wt % of 20 nm TiO<sub>2</sub> and 1 wt % of 20 nm SiO<sub>2</sub>**

Input Parameters	Symbols	Units	1 wt % of 20 nm TiO <sub>2</sub>	1 wt % of 20 nm SiO <sub>2</sub>
Specific heat capacity	$c_p$	J/kg-K	658.1323	628.694
Density	$\rho$	(kg/m <sup>3</sup> )	44.31665	24.016
Thermal conductivity	$k$	W/m-K	0.5638	0.555
Viscosity	$\nu$	Kg/ms	.00853	.00847

The discrete flow domain has been defined under sufficient limits. Inlets were allocated the mass flow rate requirements, while pressure outlet limits were allocated for outlets. The surfaces of the heat exchanger is regarded as normal wall limits. The interior walls were fitted with couplings of thermal walls.

**Table 4. Details of boundary conditions.**

Detail	Value
Molten salt nanofluid flow rate	At different Reynold's no. 15000, 35000, and 50,000
Molten salt nanofluid inlet velocity	1.2 m/s, 2.6 m/s, 3.9 m/s
Molten salt nanofluid inlet temperature	300 °C
Water (base fluid) inlet temperature	450 °C
Outer surfaces	Heat flux = 0

## IV. RESULTS AND DISCUSSIONS

This section is aimed at evaluating the heat exchanger thermal performance using nanofluids. The variations in the Heat transfer rate and Thermal conductance are measured at different Reynold's number in order to research the performance of the heat exchanger using nanofluids subject to flow

### 4.1. Data reduction equations

The values of Nusselt number, and Heat transfer coefficient calculated from the CFD modeling On the basis of temperature of hot and cold fluid obtained were compared with the values obtained from the analysis performed by **Hu Chen et al. (2020)**.

The data reduction of the measured results is summarized in the following procedures:

The Reynolds number is given by,

$$Re = \frac{\rho V D}{\mu}$$

The mass flow rate is calculate on the basis of below formula,

$$\dot{m} = \rho A V$$

Where,  $\rho$  is the density of fluid,  $A$  is the cross sectional area of the pipe and  $V$  is the velocity of fluid.

Therefore, for fluid flows in a concentric tube heat exchanger, the heat transfer rate of the hot fluid in the outer tube can be expressed as:

$$q_h = \dot{m}_h c_{ph} (T_{hi} - T_{ho})$$

Where  $\dot{m}_h$  is the mass flow rate of hot fluid,  $c_{ph}$  is the specific heat of hot fluid,  $T_{hi}$  and  $T_{ho}$  are the inlet and outlet temperatures of hot fluid, respectively.

While, the heat transfer rate of the cold fluid in the inner tube can be expressed as:

$$q_c = \dot{m}_c c_{pc} (T_{co} - T_{ci})$$

Average heat transfer rate is given by:

$$Q_{avg} = \frac{q_h + q_c}{2} = UA\theta_m$$

Where,

$$\theta_m = \frac{\theta_1 - \theta_2}{2}$$

$\theta_m$  is the logarithmic mean temperature difference.

$U$  is the overall heat transfer coefficient.

#### 4.2. Validation of numerical computations

To validate the accuracy of developed numerical approach, comparison was made with the work reported in **Patricia Anne D. Cruz, Ed-Jefferson E. Yamat et al. (2022)**. The heat exchanger geometry that used for validation of numerical computations was considered as same.

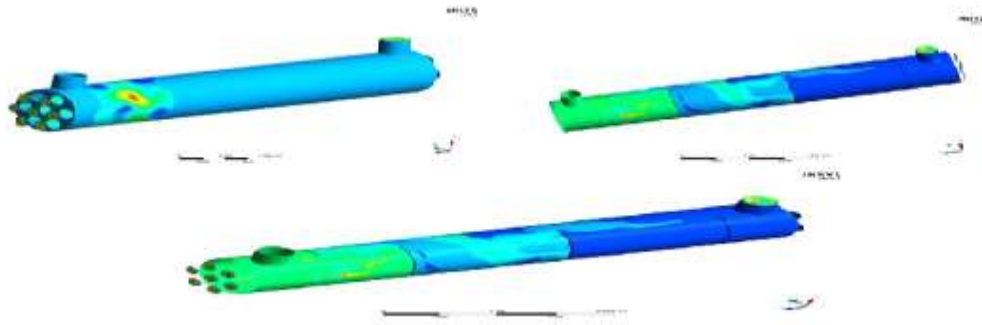


Figure 4. Temperature contour for using molten salt nanofluid with 1 wt % of 20 nm SiO<sub>2</sub> at different Reynold number (Re = 15000,35000,50000).

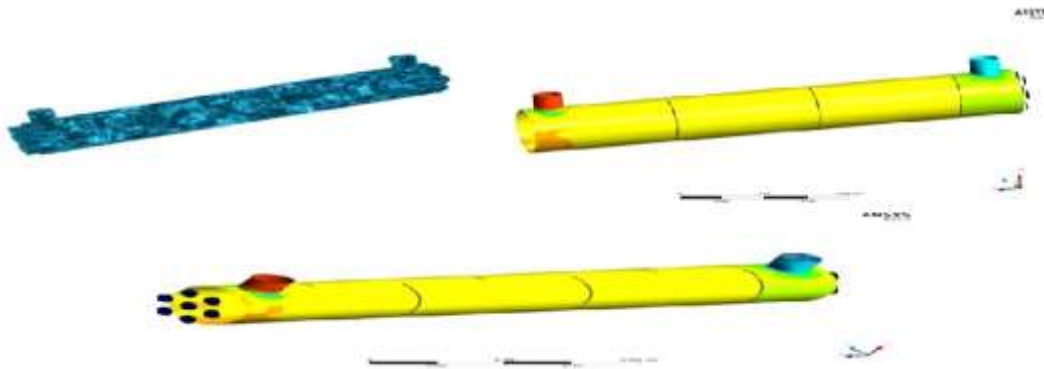


Figure 5. Pressure contour for using molten salt nanofluid with 1 wt % of 20 nm SiO<sub>2</sub> at different Reynold number (Re = 15000,35000,50000).

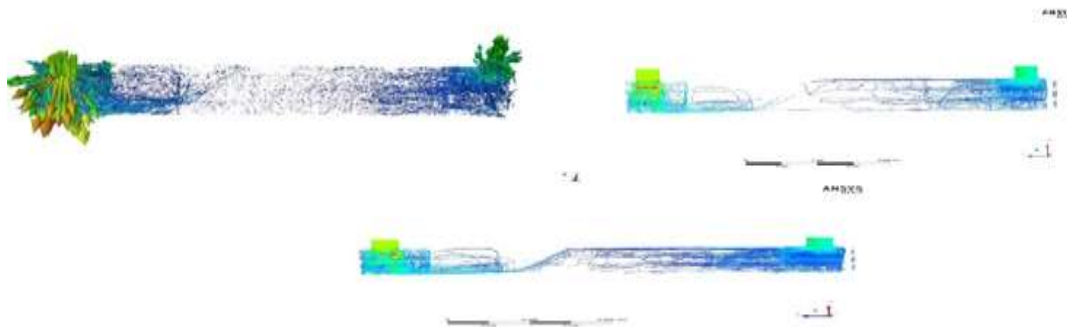


Figure 6. Velocity contour for using molten salt nanofluid with 1 wt % of 20 nm SiO<sub>2</sub> at different Reynold number (Re = 15000,35000,50000).

Now, Calculate the temperature, velocity, and temperature for the different Reynolds no. & find the value of Nusselt number using KNO<sub>3</sub>-Ca (NO<sub>3</sub>)<sub>2</sub> + TiO<sub>2</sub> molten salt nanofluid in a circular tube with the help of CFD

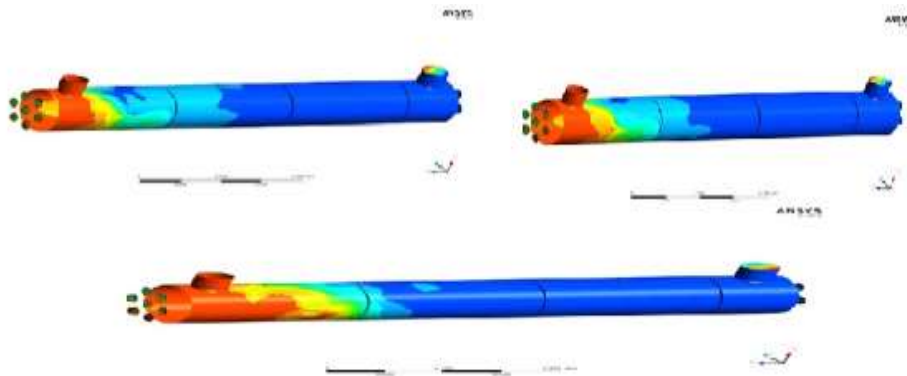


Figure 7. Temperature contour for using molten salt nanofluid with 1 wt % of 20 nm TiO<sub>2</sub> at different Reynold number (Re = 15000,35000,50000).

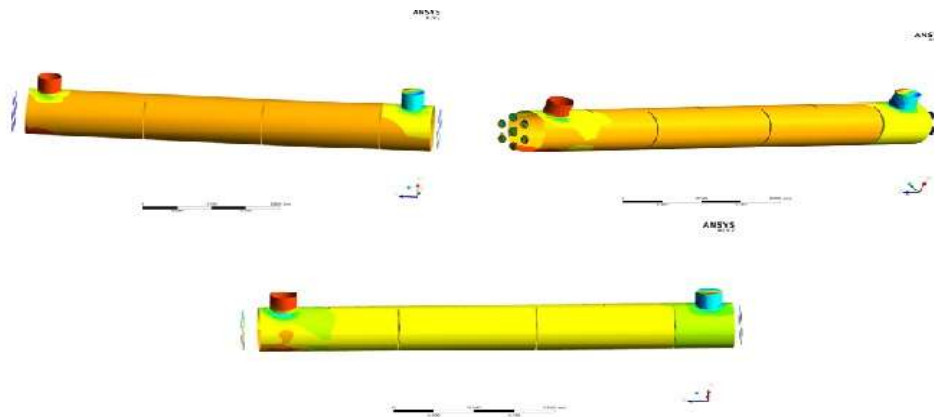


Figure 8. Pressure contour for using molten salt nanofluid with 1 wt % of 20 nm TiO<sub>2</sub> at different Reynold number (Re = 15000,35000,50000).

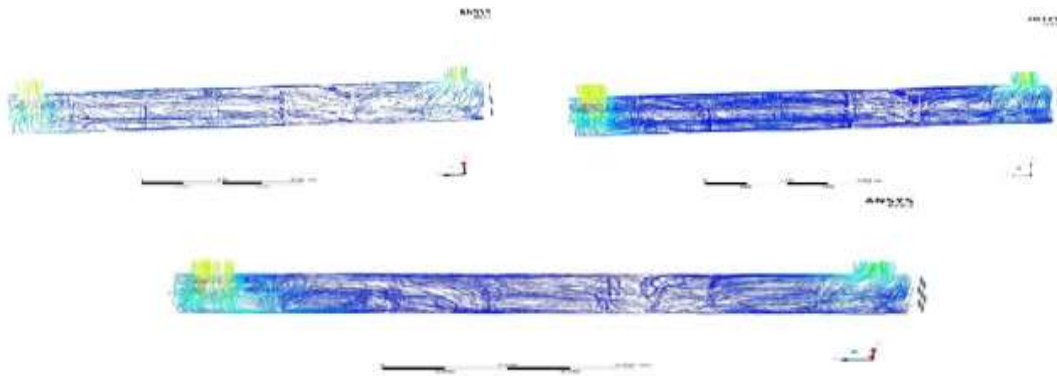


Figure 9. Velocity contour for using molten salt nanofluid with 1 wt % of 20 nm TiO<sub>2</sub> at different Reynold number (Re = 15000,35000,50000).

Calculate & Comparison of Nusselt number values for Nanofluid fluid i.e. SiO<sub>2</sub>/Molten Salt and TiO<sub>2</sub>/Molten salt at different Reynold's number

**Table 5. Values of Nusselt number at the different Reynold number**

Reynold's number	Nusselt Number	
	KNO <sub>3</sub> -Ca (NO <sub>3</sub> ) <sub>2</sub> + SiO <sub>2</sub>	KNO <sub>3</sub> -Ca (NO <sub>3</sub> ) <sub>2</sub> + TiO <sub>2</sub>
15000	116.46	133.09
35000	123.009	148.14
50000	146.46	164.46

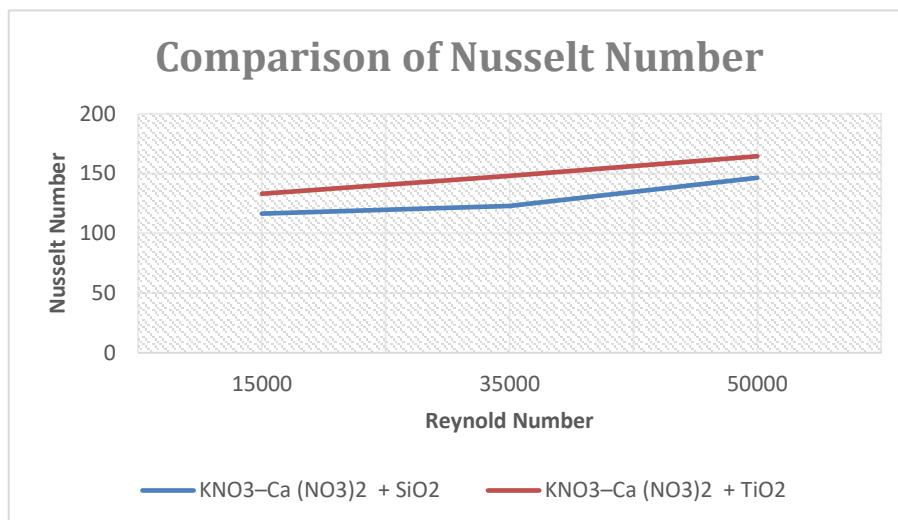


Figure 10. Nusselt number values comparison for Nanofluid i.e. SiO<sub>2</sub>/Molten Salt and TiO<sub>2</sub>/Molten salt at different Reynold's number. From the above graph, it is found that the value of Nusselt number of KNO<sub>3</sub>-Ca(NO<sub>3</sub>)<sub>2</sub> + TiO<sub>2</sub> having better than the KNO<sub>3</sub>-Ca(NO<sub>3</sub>)<sub>2</sub> + SiO<sub>2</sub>.

## V. CONCLUSIONS

The thermal characteristics of molten salt nanofluid in a circular tube are examined in this CFD research. There was strong agreement between the findings of this investigation and the most recent experimental findings reported in the literature. Testing and observation were done to determine how nanofluid affected fluid flow and heat transfer in a heat exchanger. The following inferences can be made in light of the results:

- The molten salt TiO<sub>2</sub> nanofluid outperformed the molten salt SiO<sub>2</sub> nanofluid in forced convection heat transfer under the same operating conditions.
- The Nusselt number of molten salt TiO<sub>2</sub> nanofluid was 13.46% higher than that of molten salt SiO<sub>2</sub> nanofluid.
- Additionally, it was discovered that molten salt TiO<sub>2</sub> nanofluid with a 16.96% Nusselt number at 35000 Reynolds number had a higher value than usual.

## References

- 1) Patricia Anne D. Cruz a , Ed-Jefferson E. Yamat 2022, Computational Fluid Dynamics (CFD) analysis of the heat transfer and fluid flow of copper (II) oxide-water nanofluid in a shell and tube heat exchanger (2022) 100014.
- 2) Anbumeenakshi, C. Thansekhar, M.R. , 2017. On the effectiveness of a nanofluid cooled microchannel heat sink under non-uniform heating condition. *Appl. Therm. Eng.* 113, 1437–1443.
- 3) Tiwari, A.K. , Ghosh, P. , Sarkar, J. , 2015. Particle concentration levels of various nanofluids in plate heat exchanger for best performance. *Int. J. Heat Mass Transf.* 89, 1110–1118 .
- 4) Pantzali, M.N. , Mouza, A.A , Paras, S.V. , 2009. Investigating the efficacy of nanofluids as coolants in plate heat exchangers (PHE). *Chem. Eng. Sci.* 64, 3290–3300
- 5) Teng, T.P. , Hung, Y. , Jwo, C. , Chen, C. , Jeng, L.Y. , 2011. Pressure drop of TiO<sub>2</sub> nanofluid in circular pipes. *Particuology* 9, 486–491 .
- 6) Jokar, A. , O'Halloran, S.P. , 2013. Heat transfer and fluid flow analysis of nanofluids in corrugated plate heat exchangers using computational fluid dynamics simulation. *J. Therm. Sci. Eng. Appl.* 5, 1–10 .
- 7) Devi, K.M. , Nagamani, G.V. , 2015. Design and thermal analysis of shell and tube heat exchanger by using fluent tool. *Int. J. Mag. Eng. Technol. Manag. Res.* 2, 359–366.
- 8) Azad, A. , Azad, N.V. , 2016. Application of nanofluids for the optimal design of shell and tube heat exchangers using genetic algorithm. *Case Stud. Therm. Eng.* 8, 198–206.
- 9) Masilungan-Manuel, J.T., Manuel, M.C. , Lin, P.T. , Soriano, A.N. , 2015. Optimization of the drying parameters for the short-form spray dryer producing powdered egg with 20% tapioca starch additive. *Adv. Mech. Eng.* 7, 1–11.
- 10) Ozden, E. , Tari, I. , 2010. Shell side analysis of a small shell-and-tube heat exchanger. *Energy Convers. Manag.* 51, 1004–1014.
- 11) Sitprasert, C. , Dechaumphai, P. , Juntasaro, V. , 2009. A thermal conductivity model for nanofluids including effect of the temperature-dependent interfacial layer. *J. Nanopart. Res.* 11, 1465–1476.

- 12) Haghghi, E.B. , 2015. Single Phase Convective Heat Transfer with Nanofluids–An Experimental Approach. Royal Institute of Technology, Stockholm, Sweden Doctoral Thesis .
- 13) Jadhav, A.D. , Koli, T.A. , 2014. CFD Analysis of Shell and Tube Heat Exchanger to study the effect of baffle cut on the pressure drop. *Int. J. Res. Aeronaut. Mech. Eng.* 2, 1–7 .
- 14) Rehman, U.U. , 2011. Heat Transfer Optimization of Shell-and-Tube Heat Exchanger through CFD Studies. Chalmers University of Technology, Goteborg, Sweden Master’s Thesis
- 15) Teng, T.P. , Hung, Y. , Jwo, C. , Chen, C. , Jeng, L.Y. , 2011. Pressure drop of TiO<sub>2</sub> nanofluid in circular pipes. *Particuology* 9, 486–491.
- 16) Lu, J., He, S., Ding, J., Yang, J., Liang, J., 2013. Convective heat transfer of high temperature molten salt in a vertical annular duct with cooled wall. *Appl. Therm. Eng.* 73, 1519–1524.
- 17) Chen, Y.S., Wang, Y., Zhnag, J.H., Yuan, X.F., Tian, J., Tang, Z.F., Zhu, H.H., Fu, Y., Wang, N.X., 2016. Convective heat transfer characteristics in the turbulent region of molten salt in concentric tube. *Appl. Therm. Eng.* 98, 213–219.
- 18) Du, B.-C., He, Y.-L., Wang, K., Zhu, H.-H., 2017. Convective heat transfer of molten salt in the shell-and-tube heat exchanger with segmental baffles. *Int. J. Heat Mass Transf.* 113, 456–465.
- 19) [Yanwei Hu](#), [Yurong He](#), [Zhenduo Zhang](#), [Baocheng Jiang](#), [Yimin Huang](#), 2017. Natural convection heat transfer for eutectic binary nitrate salt based Al<sub>2</sub>O<sub>3</sub> nanocomposites in solar power systems. [Renewable Energy Volume 114, Part B](#), December 2017, Pages 686-696.
- 20) Qian, J., Kong, Q.-L., Zhang, H.W., Zhu, Z.H., Huan, W.G., Li, W.H., 2017. Experimental study of shell-and-tube molten salt heat exchangers. *Appl. Therm. Eng.* 616–623